Selected Problems for Photon Colliders

*I. F. Ginzburg**

Sobolev Institute of Mathematics and Novosibirsk State University, Novosibirsk, Russia

DOI: http://dx.doi.org/10.3204/DESY-PROC-2009-03/Ginzburg

The increase of energy of Photon Colliders up to 1-2 TeV in c.m.s. offers opportunity to study new series of fundamental physical problems. Among them – multiple production of gauge bosons, hunt for strong interaction in Higgs sector, search of exotic interactions in the process $\gamma\gamma \to \gamma\gamma$ with final photons having transverse momentum $\sim (0.5 \div 0.7)E_e$.

1 Introduction

Photon Colliders (PLC) of next generation have c.m.s. energy 1-2 TeV (ILC2, CLIC,...). There are two ways of building such collider.

• The first way is to use classical conversion scheme [1] with infrared laser or FEL to reach the highest luminosity. The laser photon energy will be 0.5-0.2 eV with $x = 4.8$ which prevents pair production in collision of high energy and laser photons. In this case maximum photon energy $\omega_m \approx 0.8E$, where E is the initial electron beam energy. To get high conversion coefficient, the conversion process has to take place with large non-linear QED effects, making final photon distributions less monochromatic and less polarized. Here one must work with infrared optics which causes additional difficulties (see discussion e.g. in [2]).

• The second way is to use the same laser (and the same optics) as for the electron beam energy 250 GeV (ILC1) but limit ourselves by a small conversion coefficient $k \le 0.14$ [3]. This value assures that the losses of high energy photons due to e^+e^- pair production in collision of high energy photon with laser photon are small. At this value of conversion coefficient the non-linear QED effects are insignificant. Here the maximum photon energy is higher than in the first way, $\omega_m \approx (0.9-0.95)E$, energy distribution of high energy photons is more sharp, etc. These advantages allow to consider this option despite the reduction of $\gamma\gamma$ luminosity by about one order in comparison with the first way. Below I will have in mind these both ways. The second way seems more attractive to me. In the numerical estimates we have in mind $e\gamma$ and $\gamma\gamma$ luminosity integrals of about 100 fb^{-1} per year.

The standard list of problems for PLC at ILC1 is widely discussed (see e.g. [4]). The study of some of them (with increase of thresholds for search of new particles) will be a natural task for PLC with higher beam energy. We discuss here some new opportunities provided to us by enhancement of beam energy.

*This research has been supported by Russian grants RFBR 08-02-00334-a and NSh-1027.2008.2.

2 Multiple production of SM gauge bosons

The observation of pure interactions of SM gauge bosons (W and Z) or their interaction with leptons will allow to check SM with higher accuracy and observe signals of New Physics. The most ambitious goal is to find deviations from predictions of SM caused by New Physics interactions (and described by anomalies in effective Lagrangian). There are many anomalies relevant to the gauge boson interactions. Each process is sensitive to some group of anomalies. Large variety of processes obtainable at PLC's allows to separate anomalies from each other. The high energy PLC is the only collider among different future accelerators where one can measure large number of different processes of such type with high enough accuracy.

2-nd order processes. The cross sections of basic processes $\gamma\gamma \to W^+W^-$ and $e\gamma \to \nu W$ are so high (Fig. 1) that one can expect to obtain about 10^7 events per year providing accuracy better than 0.1%. The cross sections are almost independent of energy and photon polarization [5]. However, final distributions depend on polarization strongly [7].

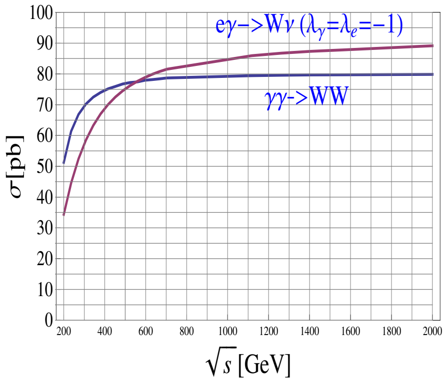

Figure 1: *Cross sections of 2-nd order processes*

The accuracy of measurement of these cross sections is sufficient to study in detail 2-loop radiative corrections. Together with standard problems of precise calculations one can note here two non-trivial problems, demanding detailed theoretical study:
(i) construction of S–matrix for system with unstable particles;
(ii) gluon corrections like Pomeron exchange between quark components of W's.

The mentioned high values of cross sections of the 2-nd order processes make it possible to measure their multiple "radiative derivatives" — processes of the 3-rd and 4-th order, depending in different ways on various anomalous contributions to the effective Lagrangian.

3-rd order processes. We consider here 3 processes. Total cross section $\sigma_{e\gamma\to eWW} \simeq$

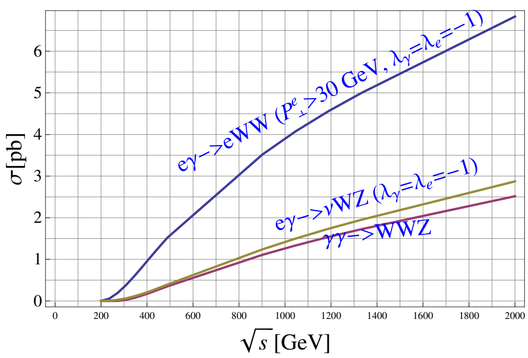

Figure 2: *Cross sections of 3-rd order processes*

$dn_\gamma \otimes \sigma_{\gamma\gamma\to WW}$. It is very high and easily estimated by equivalent photon method. This large contribution is not very interesting, being only a cross section of $\gamma\gamma \to W^+W^-$ averaged with some weight. However, at large enough transverse momentum of scattered electron this factorization is violated. Because of it we present $\sigma_{e\gamma\to eWW}$ only for $p_{\perp e} > 30$ GeV. Even this small fraction of total cross section appears so large that it allows *to separate contribution of* $\gamma Z \to WW$ *subprocess.*

4-th order processes. The cross sections of these processes (Fig. 3) are high enough to measure them with 1% precision. For the same reason as for process $e\gamma \to eWW$ we present cross section for process $e\gamma \to eZWW$ only for $p_{\perp e} > 30$ GeV. Even this small fraction of total cross section appears so large that it allows *to separate contribution of* $\gamma Z \to WWZ$ *subprocess.*

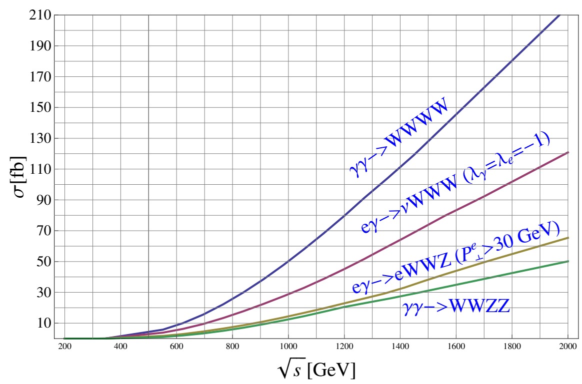

Figure 3: *Cross sections of 4-th order processes*

The study of the 2-nd order processes will allow to extract some anomalous parameters or their combinations. The study of the 3-rd order processes will allow to enlarge the number of extracted anomalous parameters and separate some of combinations extracted from the 2-nd order processes. The study of the 4-th order processes will again enlarge the number of separated anomalous parameters.

3 Study of strong interaction in Higgs sector

It is well known that at high values of Higgs boson self-coupling constant, the Higgs mechanism of Electroweak Symmetry Breaking in Standard Model (SM) can be realized without actual Higgs boson but with strong interaction in Higgs sector (SIHS) which will manifest itself as a strong interaction of longitudinal components of W and Z bosons. It is expected that this interaction will be similar to the interaction of π-mesons at $\sqrt{s} \lesssim 1.5$ GeV and will be seen in the form of W_LW_l, W_LZ_L and Z_LZ_L resonances. Main efforts to discover this opportunity are directed towards the observation of such resonant states. It is a difficult task for the LHC due to high background and it cannot be realized at the energies reachable at the ILC in its initial stages.

The problem of discovery of this strong interaction can be solved in the study of the charge asymmetry of produced $W^\pm$ in the process $e^-\gamma \to e^-W^+W^-$ similar to that which was discussed in low energy pion physics [8], [9]. To explain the set up of the problem we will discuss this process in SM.

We subdivide the diagrams of the process into three groups, where subprocesses of main interest are shown in boxes, sign $\otimes$ represents next stage of process and sign $\oplus$ represents adding of photon line to each charged line for subprocess in box:

$$\begin{aligned} &a) \quad e^- \to e^-\gamma^*(Z^*) \otimes \boxed{\gamma\gamma^*(Z^*) \to W^+W^-};\\ &b) \quad \gamma e^- \to e^{-*} \to e^-\gamma^*(Z^*) \otimes \boxed{\gamma^*(Z^*) \to W^+W^-};\\ &c) \quad \gamma \oplus \boxed{e^- \to W^-W^+e^-}. \end{aligned} \tag{1}$$

Diagrams of type a) contain subprocesses $\gamma\gamma^* \to W^+W^-$ and $\gamma Z^* \to W^+W^-$, modified by the strong interaction in the Higgs sector (*two–gauge contribution*).

Diagrams of type b) contain subprocesses $\gamma^* \to W^+W^-$ and $Z^* \to W^+W^-$, modified by the strong interaction in the Higgs sector (*one–gauge contribution*).

Diagrams of type c) are made by connecting the photon line to each charged particle line to the diagram shown inside the box. Strong interaction does not modify this contribution. These contributions are switched off at suitable electron polarization.

The subprocess $\gamma\gamma^* \to W^+W^-$ (from contribution a)) produces C-even system W^+W^-, the subprocess $\gamma^* \to W^+W^-$ (from contribution b)) produces C-odd system W^+W^-. The interference of similar contributions for the production of pions is responsible for large enough charge asymmetry, very sensitive to the phase difference of S (D) and P waves in $\pi\pi$ scattering, [8]. This very phenomenon also takes place in the discussed case of W's. However, for the production of $W^\pm$ subprocesses with the replacement of $\gamma^* \to Z^*$ are also essential. Therefore, the final states of each type have no definite C-parity. Hence, charge asymmetry appears both due to interference between contributions of types a) and b) and due to interference of γ^* and Z^* contributions each within their own types, like charge asymmetry in e^+e^- collision near $Z-$ peak.

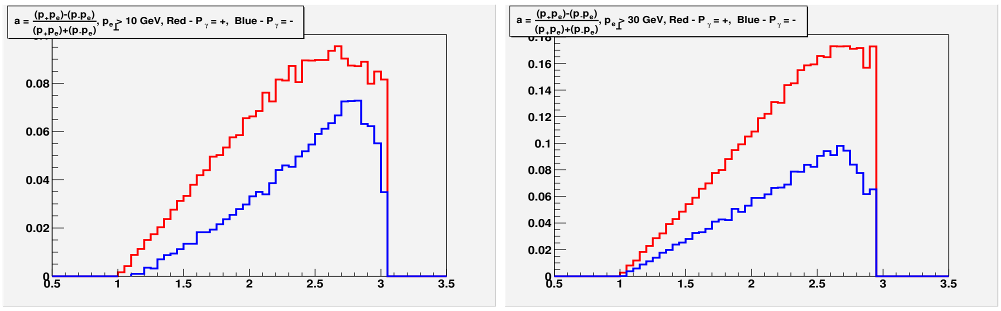

Figure 4: Dependence on polarization and cuts. Variable v_1.

Asymmetries in SM. To observe the main features of the effect of charge asymmetry and its potential for the study of strong interaction in the Higgs sector, we calculated some quantities describing charge asymmetry (charge asymmetric variables – CAV) for $e^-\gamma$ collision at $\sqrt{s} = 500$ GeV with polarized photons. We used CompHEP and CalcHEP packages [10] for simulation.

Denoting by $p^\pm$ momenta of $W^\pm$, by p_e – momentum of the scattered electron and by $W = \sqrt{(p_e^+ + p_e^-)^2}$, we studied W-dependence of the following averaged quantities

$$v_1 = \frac{\langle (p^+ - p^-)p_e \rangle}{\langle (p^+ + p^-)p_e \rangle}\,, \qquad v_2 = \frac{\langle (p_\parallel^+)^2 - (p_\parallel^-)^2 \rangle}{\langle (p_\parallel^+)^2 + (p_\parallel^-)^2 \rangle}\,, \qquad v_3 = \frac{\langle (p_\perp^+)^2 - (p_\perp^-)^2 \rangle}{\langle (p_\perp^+)^2 + (p_\perp^-)^2 \rangle}\,. \tag{2}$$

We applied the cut in transverse momentum of the scattered electron,

$$p_\perp^e \ge p_{\perp 0} \quad \text{with} \quad \begin{cases} a)\ p_{\perp 0} = 10\ GeV, \\ b)\ p_{\perp 0} = 30\ GeV. \end{cases} \tag{3}$$

Observation of the scattered electron allows to check kinematics completely.

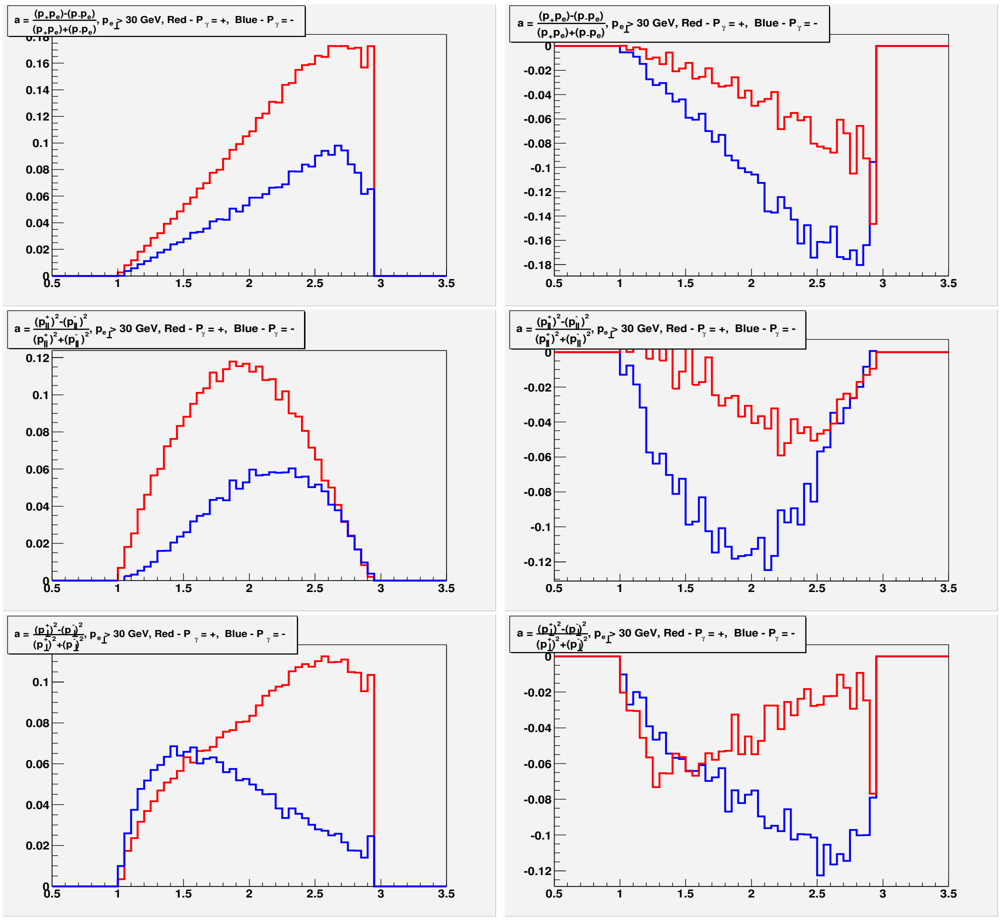

Figure 5: *Asymmetries in variables v_1, v_2 and v_3 (from top to bottom). Right – total, left – without one-gauge contributions. Upper curves for the right–handed polarized photons, lower curves for the left–handed polarized photons.*

• *Influence of polarization* for the charge asymmetry. Fig. 4 represents distribution in CAV v_1 for the right-hand (upper curves) and the left-hand (lower curves) polarized photons at cuts $p_{\perp 0} = 10$ GeV (left) and $p_{\perp 0} = 30$ GeV (right). We did not study the dependence on electron polarization. This dependence is expected to be weak in SM where main contribution to cross section is given by diagrams of type a) with virtual photons having the lowest possible energy. These photons "forget" the polarization of the incident electron. The strong interaction contribution becomes essential at highest effective masses of WW system with high energy of virtual photon or Z, the helicity of which reproduces almost completely the helicity of incident electron [11]. Therefore, study of this dependence will be a necessary part of studies beyond SM.

• *Significance of different contributions.* To understand the extent of the effect of interest, we compared the entire asymmetry to that without one-gauge contribution (Fig. 5). Strong interaction in the Higgs sector modifies both one–gauge and two–gauge contributions. The study of charge asymmetry caused by their interference will be a source of information on this strong interaction. One can see that one–gauge contribution is so essential that neglecting on it even changes the sign of charge asymmetry (compared to that for the entire process).

Therefore, the influence of this potentially informative contribution to asymmetry is very high. The curves of Fig. 5 show that the value of this interference effect grows with the increase of the cut in $p_{e\perp}$. Photon polarization influences strongly the value of charge asymmetry. The role of electron polarization remains to be studied.

One can conclude that the charge asymmetry is very sensitive to the interference of two–gauge and one–gauge contributions which is modified under the strong interaction in the Higgs sector. The measurement of this asymmetry will be a source of data on the phase difference of different partial waves of $W_L W_L$ scattering.

4 Large angle high energy photons for exotics

The PLC allows to observe signals from the whole group of exotic models of New Physics in one common experiment. These are models with *large extra dimensions* [12], *point-like monopole* [13], *unparticles* [14]. All these models have common signature – the cross section for $\gamma\gamma \to \gamma\gamma$ production grows with energy as ω^6 ($\omega = \sqrt{s}/2$) and the photons are produced almost isotropically. Future observations either will give limits for scales of these exotics or will allow to see these effects by recording large $p_\perp \sim (0.5 \div 0.7)E_e$ photons[1]. The study of dependence on initial photon polarization will be useful to separate the mechanisms.

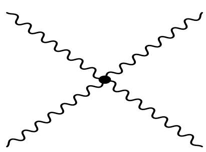

Figure 6: *Effective Lagrangian*

All these exotics at modern day energies can be described by effective point-like interaction of Fig. 6:

$$L \propto \frac{F^{\mu\nu} F^{\alpha\beta} F_{\rho\sigma} F_{\phi\tau}}{\Lambda^4}, \quad (\Lambda^2 \gg s/4). \tag{4}$$

In different models different orders of field indices are realized, Λ is characteristic mass scale, expressed via parameters of model. (In all cases s, t and u – channels are essential.)

Let us describe main features of matrix element (in the photon c.m.s.):

• gauge invariance provides factor ω for each photon leg;

• to make this factor dimensionless it should be written as ω/Λ. Therefore, the amplitude $\mathcal{M} \propto (\omega/\Lambda)^4 = s^2/(2\Lambda)^4$.

[1] *In my personal opinion it is hardly probable that these models describe reality.*

The characteristic scale Λ is large enough not to contradict modern day data. It accumulates other coefficients. The cross section

$$\sigma_{tot} = \frac{1}{32\pi s}\left(\frac{s}{4\Lambda^2}\right)^4, \quad d\sigma = \sigma_{tot}\Phi\left(\frac{p_\perp^2}{s}\right)\frac{2dp_\perp^2}{\sqrt{s(s-4p_\perp^2)}}. \tag{5}$$

with smooth function $\Phi(p_\perp^2/s)$, describing some composition of S and P-waves, dependent on details of model, and $\int \Phi(z)\dfrac{2dz}{\sqrt{1-4z}} = 1$. For large extra dimensions and monopoles entire s dependence is given by the factor $s^4/(2\Lambda)^8$ from (5), for unparticles additional factor $(s/4\Lambda^2)^{d_u-2}$ is added.

For the **large extra dimensions** case the point in Fig. 6 describes an elementary interaction, given by product of stress-energy tensors T_{ab} for the incident and the final photons, that are exchanging the tower of Kaluza-Klein excitations (with permutations),

	Λ	reference
Tevatron D0	175 GeV	[15]
LHC	2 TeV	[13]
$\gamma\gamma$ (100 fb^{-1})	$3E_e$	[13]
e^+e^- LC (1000 fb^{-1})	$2E_e$	[13]

Table 1: *The obtainable discovery limits.*

$$\mathcal{M}_{\gamma\gamma\to\gamma\gamma} \propto \left\langle\frac{T_{ab}T^{ab}}{\Lambda^4}\right\rangle \approx \frac{F^{\mu\nu}F_{\nu\alpha}F^{\alpha\beta}F_{\beta\mu}}{\Lambda^4} + \textit{permutations},$$

After averaging over polarizations for tensorial KK excitations

$$\Phi \propto 2\left(1-\frac{p_\perp^2}{\hat{s}}\right)^2 = \frac{(3+\cos^2\theta)^2}{8} = \frac{\hat{s}^4+\hat{t}^4+\hat{u}^4}{2\hat{s}^4}. \tag{6}$$

Unlike to ILC1, at high energy PLC the other channels (like $\gamma\gamma\to WW$) are less sensitive to the extra dimension effect.

The point–like Dirac monopole existence would explain mysterious quantization of an electric charge since in this case $ge = 2\pi n$ with $n = 1, 2, ...$ *There is no place for this monoplle in modern theories of our world but there are no precise reasons against its existence.* In this case the point in Fig. 6 corresponds to exchange of loop of heavy monopoles (like electron loop in QED – Heisenberg–Euler type lagrangian).

Let M be monopole mass. At $s \ll M^2$ the electrodynamics of monopoles is expected to be similar to the standard QED with effective perturbation parameter $g\sqrt{s}/(4\pi M)$ [13]. The $\gamma\gamma\to\gamma\gamma$ scattering is described by monopole loop, and it is calculated within QED,

$$\mathcal{L}_{4\gamma} = \frac{1}{36}\left(\frac{g}{\sqrt{4\pi}M}\right)^4\left[\frac{\beta_+ + \beta_-}{2}\left(F^{\mu\nu}F_{\mu\nu}\right)^2 + \frac{\beta_+ - \beta_-}{2}\left(F^{\mu\nu}\tilde{F}_{\mu\nu}\right)^2\right].$$

The coefficients $\beta_\pm$ and details of angular and polarization dependence depend strongly on the spin of the monopole.

After averaging over polarizations, the $p_\perp$ dependence and total cross section are described by the same equations as for the extra dimensions case. The parameter Λ is expressed via monopole mass and coefficient a_J, dependent on monopole spin J ($n = 1, 2, ...$):

$$\Lambda = (M/n)a_J, \quad \textit{where} \quad a_0 = 0.177, \ a_{1/2} = 0.125, \ a_1 = 0.069. \tag{7}$$

Unparticle $\mathcal{U}$ is an object, describing particle scattering via propagator which has no poles at real axis. It was introduced in 2007 [14]. This propagator behaves (in the scalar case) as

$(-p^2)^{d_U-2}$ where scalar dimension d_u is not integer or half-integer. The interaction carried by unparticle is described as $\dfrac{F^{\mu\nu}F_{\mu\nu}\mathcal{U}}{\Lambda^{2d_U}}$ with some phase factor. For matrix element it gives

$$\mathcal{M} = \frac{F^{\mu\nu}F_{\mu\nu}F^{\rho\tau}F_{\rho\tau}}{\Lambda^{4d_U}}(-P^2)^{d_U-2} \; + \; permutations\,.$$

$$|\mathcal{M}|^2 = C\frac{s^{2d_U} + |t|^{2d_U} + |u|^{2d_U} + \cos(d_u\pi)[(s|t|)^{d_U} + (s|u)^{d_U}] + (tu)^{d_U}}{\Lambda^{4d_U}}$$

The expected discovery limits for all these models are shown in the Table 1. The results of D0 experiment [15], recalculated to used notations, are also included here. For the unparticle model presented numbers are modified by corrections $\propto (d_U - 2)$.

References

[1] I.F. Ginzburg, G.L. Kotkin, V.G. Serbo, V.I. Telnov. *Nucl. Instr. Meth.* **205** (1983) 47–68; I.F. Ginzburg, G.L. Kotkin, S.L. Panfil, V.G. Serbo, V.I. Telnov. *Nucl. Instr. Meth.* **219** (1983) 5.

[2] V. Telnov. hep-ex/0012047

[3] I.F. Ginzburg, G.L. Kotkin, V.G. Serbo, in preparation

[4] B. Badelek et al. *TESLA TDR* hep-ex/0108012

[5] I.F. Ginzburg, G.L. Kotkin, S.L. Panfil, V.G. Serbo. *Nucl. Phys.* **B228** (1983) 285

[6] I.F. Ginzburg, V.A.Ilyin, A.E.Pukhov, V.G.Serbo, S.A.Shichanin. *Phys. At. Nucl.– Russian Yad Fiz.* **56** (1993) 57–63.

[7] D. A. Anipko, I. F. Ginzburg, K.A. Kanishev, A. V. Pak, M. Cannoni, O. Panella. *Phys. Rev.* **D 78** (2008) 093009; ArXive: hep-ph/0806.1760

[8] V.L. Chernyak, V.G. Serbo, *Nucl. Phys.* **B 67** (1973) 464;
I.F.Ginzburg, A.Schiller, V.G. Serbo, *Eur. Phys. J.* **C18** (2001) 731

[9] I.F.Ginzburg, *Proc. 9th Int. Workshop on Photon-Photon Collisions*, San Diego (1992) 474

[10] E. Boos et al. *Nucl. Instr. Meth.* **A534** (2004) 250; A. Pukhov. hep-ph/0412191

[11] I.F. Ginzburg, V.G. Serbo. *Phys. Lett.* **B 96** (1980) 68-70.

[12] K.R. Dienes, E. Dudas, T. Gherghetta. hep-ph/9803466, *Phys. Lett.* **B 436** (1998); M. Shifman. hep-ph/09073074

[13] I.F. Ginzburg, S.L. Panfil. Sov. Yad. Fiz. **36** (1982) 850; I.F. Ginzburg, A. Schiller. *Phys. Rev.* **D 60** (1999) 075016

[14] H. Georgy, *Phys. Rev. Let.* **98** (2007) 221601;hep-ph/0703.260; I.Sahin, S.C. Inan hep-ph/09073290

[15] B. Abbot et al. *Phys. Rev. Lett.* **81** (1998) 524, hep-ex/9803023